Laboratory Investigation (2010), 1–14

TNF gene cluster deletion abolishes lipopolysaccharide-mediated sensitization of the neonatal brain to hypoxic ischemic insult

Giles S Kendall[1], Mariya Hirstova[1], Sigrun Horn[2], Dimitra Dafou[3], Alejandro Acosta-Saltos[1], Beatriz Almolda[4], Virginia Zbarsky[1], Prakasham Rumajogee[1], Heike Heuer[2], Bernardo Castellano[4], Klaus Pfeffer[5], Sergei A Nedospasov[6], Donald M Peebles[1] and Gennadij Raivich[1]

In the current study, we explored the role of TNF cluster cytokines on the lipopolysaccharide (LPS)-mediated, synergistic increase in brain injury after hypoxic ischemic insult in postnatal day 7 mice. Pretreatment with moderate doses of LPS (0.3 μg/g) resulted in particularly pronounced synergistic injury within 12 h. Systemic application of LPS alone resulted in a strong upregulation of inflammation-associated cytokines TNFα, LTβ, interleukin (IL) 1β, IL6, chemokines, such as CXCL1, and adhesion molecules E-Selectin, P-Selectin and intercellular adhesion molecule-1 (ICAM1), as well as a trend toward increased LTα levels in day 7 mouse forebrain. In addition, it was also associated with strong activation of brain blood vessel endothelia and local microglial cells. Here, deletion of the entire TNF gene cluster, removing TNFα, LTβ and LTα completely abolished endotoxin-mediated increase in the volume of cerebral infarct. Interestingly, the same deletion also prevented endothelial and microglial activation following application of LPS alone, suggesting the involvement of these cell types in bringing about the LPS-mediated sensitization to neonatal brain injury.
Laboratory Investigation advance online publication, 6 December 2010; doi:10.1038/labinvest.2010.192

KEYWORDS: encephalopathy; hypoxia; inflammation; ischemia; neonate; TNF

Although bacteria and viruses can directly infect and injure developing brain, infections occurring outside the brain frequently will also have a damaging effect. Congenital infections appear to contribute up to 5% of cerebral palsy cases[1,2] and may sensitize the brain to perinatal hypoxic ischemic (HI) insult.[3–5] This synergistic effect was also reproduced in mammalian and avian animal models, combining HI insult and the lipopolysaccharide break-down product of bacteria in HI animal models.[6–10] However, the molecular mediators of this endotoxin effect *in vivo* are currently still unknown.

Both *in vitro* and *in vivo* studies show that endotoxin will upregulate numerous cytokines and chemokines,[11] upregulate signaling enzymes, such as inducible nitrogen oxide synthase (iNOS), and cyclo-oxygenase-2 (COX2) and enhance the expression of adhesion molecules on parenchymal microglia and the brain vascular endothelium.[12–15] Follow on molecular studies reveal that these effects are transmitted through the classical endotoxin receptors, primarily the toll-like receptor 4 (TLR4), on blood vessel endothelia and microglia,[16,17] and involve MyD88 and NF-kappa-B components of the innate immunity cascade.[17] In particular, endotoxin-induced pro-inflammatory cytokines, including TNFα and interleukin 1β (IL1β) are known to have a number of deleterious effects, including a direct toxic effect on neurones and vulnerable oligodendrocyte precursors,[18,19] astrogliosis with release of nitric oxide, and mitochondrial dysfunction,[20] as well as microglial activation with release of nitric oxide, superoxide and a panel of other inflammation-associated molecules.[19,21,22]

[1]Perinatal Brain Repair Group, Centre for Perinatal Brain Protection and Repair, Institute of Women's Health, University College London, London, UK; [2]Neuroendocrinology Research Group, Leibniz Institute for Age Research-Fritz-Lipmann-Institute, Jena, Germany; [3]Department of Medical and Molecular Genetics, Guy's Hospital, King's College, London, UK; [4]Department Cell Biology, Physiology and Immunology, Autonomous University of Barcelona, Barcelona, Spain; [5]Institute of Medical Microbiology, University of Düsseldorf, Düsseldorf, Germany and [6]Molecular Immunology Lab, Engelhardt Institute of Molecular Biology, Russian Academy of Sciences, Moscow, Russia
Correspondence: Dr GS Kendall, BSc(hons), MBBS, MRCPCH, PhD, Perinatal Brain Repair Group, Centre for Perinatal Brain Protection and Repair, Institute of Women's Health, University College London, 86-96 Chenies Mews, London WC1E 6HX, UK.
E-mail: g.kendall@ucl.ac.uk

Received 29 June 2010; revised 4 October 2010; accepted 20 October 2010; published online 6 December 2010

TNFα along with lymphotoxin (LT)-α, and LTβ form a subfamily within a larger family of TNF-related ligands. These three cytokines have their genes linked within a compact 12-kb cluster inside the major histocompatibility complex, and demonstrate a number of overlapping functions acting through common receptors.[23,24] There are several lines of evidence that suggest the involvement of the TNF cytokine cluster group. Children who develop cerebral palsy show raised blood levels of TNFα,[25] as well as enhanced association with single-nucleotide polymorphism for LTα.[26] Moreover, both TNFα and LTα, signal through TNF receptor 1,[27] which appears critical for endotoxin-mediated sensitization to oxygen glucose deprivation *in vitro*.[28]

In the current study we, therefore, explored the effects of the TNF gene cluster cytokines TNFα, LTα and LTβ on endotoxin-mediated sensitization to HI insult in the neonatal mouse, and associated cellular activation and molecular changes using complete deletion of the TNF cluster, pretreatment with endotoxin and the Rice-Vannucci model of unilateral occlusion of left common carotid artery and 30-min hypoxia in 8% oxygen.[29] Our results show that the TNF cluster cytokines are upregulated by endotoxin *in vivo*, that their deletion prevents the normally observed microglial and vascular activation following application of endotoxin alone, and that the TNF cluster null mice also no longer exhibit the endotoxin-mediated sensitizing effect on HI insult.

MATERIALS AND METHODS

Animals

The animal experiments and care protocols were approved by the Home Office and were carried out according to the UK Animals (Scientific Procedures) Act 1986. All experiments were performed on mice at postnatal day 6–7 (P6-7) bred in house. Wild-type animals were the offspring of C57/Bl6 female (Charles River, Kent, UK) and males (Harlan, Oxfordshire, UK). Animals homozygous for a deletion of the entire TNF cluster were provided by K Pfeffer Institute of Medical Microbiology, University of Dusseldorf, Dusseldorf, Germany. The generation and phenotypic analysis of these mice with combined TNFα/LTα/LTβ deficiency has been previously described.[23] These animals were back crossed with C57/Bl6 (Charles River) for four generations; heterozygote animals from F_4 were then bred and their offspring used for the study.

HI Insult and Endotoxin

Animals at P7 were anaesthetized with isofluorane (5% induction 1.5% maintenance), the left common carotid artery permanently occluded with 8/0 polypropylene suture and the wound closed with tissue glue. The mice were recovered at 36°C, returned to the dam for 2 h, and then placed in a hypoxia chamber and exposed to humidified 8% oxygen/92% nitrogen (2 l/min) at 36°C for 30 min.

For the endotoxin experiments, lipopolysaccharide (LPS) from *Escherichia coli*, serotype 055:B5 (Fluka) was dissolved in sterile normal saline. A single intraperitoneal injection at dose of 0.3–20 μg/g body weight was given either alone or 0–24 h before surgery. LPS injections were diluted in saline so that all animals received a single 10 μl/g injection. Control animals received 10 μl/g sterile normal saline.

Histochemistry and Immunohistochemistry

For histological assessment, animals were killed by intraperitoneal injection of pentabarbitone and perfused with 30 ml of phosphate-buffered saline (PBS). The brains were then removed, postfixed for 1 h by rotating immersion in 4% formaldehyde (FA) in PBS at 4°C and then cryoprotected for 24 h in a phosphate-buffered 30% sucrose solution as described before.[30] Fixed cryoprotected brains were frozen on dry ice, cut on a cryostat into sequential 40-μm sections and stored at −80°C until required.

The sections were thawed and rehydrated in bidistilled water, spread onto glass slides coated with 0.5% gelatine under a dissecting microscope, dried for 5 min, fixed in 4% FA (Merck) in 100 mM phosphate buffer (PB; pH 7.4) for another 5 min, defatted in acetone (50%, 2 min; 100%, 2 min; and 50%, 2 min), washed twice in PB and then in PB with 0.1% bovine serum albumin (PB/BSA; Sigma, Deisenhofen, Germany). The acetone steps were omitted with some integrin stains shown in Table 1. Immunostainings for cyclooxygenase-2 and iNOS were performed on floating sections using a protocol with hydrogen-peroxide/methanol, followed by blocking with anti-mouse Immunoglobulin F'(ab) fragments and Triton X-100 pretreatment (Table 1).

DNA fragmentation was detected using transferase-mediated biotinylated d-UTP Nick End-Labelling (TUNEL) with terminal TUNEL using the Roche kit (Roche, West Sussex, UK); the endogenous granulocyte myeloperoxidase enzyme by the covalent binding of biotinylated tyramide (NEN, Cologne, Germany, 1% solution in PBS) for 10 min at room temperature in the presence of 0.001% hydrogen peroxide.

For routine immunohistochemistry, pretreated sections were preincubated with 5% goat serum (Sigma) in PB and then incubated with the respective primary antibody overnight at 4°C. The sections were washed (PB/BSA, PB; PB, PB/BSA), incubated with the appropriate secondary antibodies (anti-rat, anti-hamster, anti-mouse or anti-rabbit immunoglobulin, Ig) and then visualized with Avidin-Biotinylated peroxidise Complex (Vector Laboratories, Burlingame, CA, USA), and then stained with diaminobenzidine/hydrogen peroxide, processed through alcohol and xylene and embedded in DEPEX. For double labelling (Figure 6), preincubation was done with 5% donkey serum as described in Hristova *et al*,[31] the secondary antibodies included an AlexaFluor488-conjugated goat anti-rat Ig or goat anti-hamster Ig, and the staining enhanced again with a tertiary AlexaFluor488-conjugated donkey anti-goat Ig antibody and Texas Red-Avidin (1:1000 in PB/BSA; Dianova) for 2 h at room temperature.

Table 1 Summary of primary antibodies

Antigen	Primary antibody	Acetone pre-treated	Dilution
αM Integrin subunit (CD11b/18, αMβ2)	Rat anti-mouse αM (Serotec MCA711)	Yes	1:5000
αX Integrin subunit (CD11c/18, αXβ2)	Hamster anti-mouse αX (Endogen MA 11C5)	Yes	1:400
α5 Integrin subunit (CD49e/29, α5β1)	Rat anti-mouse α5 (Pharmingen 01741D)	No	1:200
α6 Integrin subunit (CD49f/29, α6β1),	Rat anti-mouse α6 (Serotec MCA699)	Yes	1:3000
Intercellular adhesion molecule-1 (CD54, ICAM1)	Hamster anti-mouse ICAM1 (Pharmingen 01541D)	Yes	1:3000
Cyclo-oxygenase-2 (COX2)	Mouse anti-mouse COX2 (BD Transduction Labs, 610329)	No[a]	1:100
Glial fibrillary acidic protein (GFAP)	Rabbit anti-cow GFAP (Dako Z0334)	Yes	1:6000
Ionized calcium-binding adaptor protein 1 (IBA-1)	Rabbit anti-mouse IBA1 (from Dr Y Imai, National Institute of Neuroscience, Japan	Yes	1:400
Inducible NO synthase (iNOS)	Mouse anti-mouse iNOS (BD Transduction Labs, 610203)	No[a]	1:1000
Vascular cell adhesion molecule-1 (VCAM1)	Rat anti-mouse VCAM1 (Serotec MCA1229)	No	1:400

[a]Tissue sections stained for COX2 and iNOS were pretreated for 10 min with 2% H_2O_2 in 70% methanol, 3 h in F′(ab) blocking solution (AffiniPure Fab fragment rabbit anti-mouse IgG; 1:100; 315-007-003; Jackson Immunoresearch Laboratories) and then for 1 h with 1% Triton X-100 in 50 mM Tris-buffered saline, pH 7.4, supplemented with 10% fetal calf serum and 3% BSA.

In Situ Hybridization (ISH)

For colocalization experiments with ISH for TNFα mRNA cryosections were first stained for the microglial marker αM as described before. To prevent RNA degradation, all incubation steps were carried out in the presence of 10 U/ml RNase Inhibitor (Ambion). Following the peroxidase staining reaction with DAB/H_2O_2 as substrates, the cytokine transcripts were then localized by ISH as described before.[31] cDNA fragments corresponding to nucleotides 946–1477 of mouse TNFα (GeneBank accession code NM_013693.2) were generated by PCR and subcloned into the pGEM-T easy vector (Promega). The same procedures were also performed for LTα (nts: 748–1171, NM_010735) and LTβ (nts: 314–903, NM_008518) ISH, but these were not associated with a visible autoradiographic signal.

DNA Isolation and Genotyping

DNA extraction from tail tips taken during perfusion was performed using the 'Wizard' Genomic DNA purification system according to manufacturer's instructions (Promega). Specific oligonucleotide primers (Invitrogen) were used for genotyping.

Wild-type forward primer: 5′-CGGGTCTCCGACCTAGAGATC-3′
reverse primer: 5′-CCCACGCTCGTGTACCATAAC-3′

Knockout forward primer: 5′-CACCCACCCCCGTTTTCTTTCTTC-3′
reverse primer: 5′-CCACTTGTCCAGTGCCTGCTC-3′

mRNA Quantification

Animals were killed by decapitation, their brains quickly removed, frozen in liquid nitrogen and kept at −80°C till processed. The left hemisphere of the forebrain was micro-dissected in the frozen state and total RNA isolated using the RNeasy minikit (Qiagen, West Sussex, UK) following needle disruption and homogenization according to the manufacturer's instructions. After phenol:chloroform extraction and column separation, the recovered RNA was reverse transcribed as described previously.[32] The transcribed cDNA was checked for integrity on gel electrophoresis and then analyzed in a TaqMan custom microarray to quantify levels of IL1β, IL6, IL10, IL12β, TNFα, TGFβ1, E-Selectin, P-Selectin, ICAM1, vascular cell adhesion molecule-1 (VCAM1) chemokine (C-X-C motif) ligand 1 (CXCL1) and chemokine (C-C motif) ligand 2 (CCL2) using custom-made amplification primers. The 'relative quantification study' programme of SDS2.1 software was used for analyzing data. First, the cycle number at which the increase in fluorescence (and therefore cDNA) became exponential (C_t) for both the target gene and the control gene (18S) were measured and the difference in C_t between the control and target gene was calculated for each well (δ C_T). The results were expressed using the comparative C_t or $2^{-[\mathrm{delta}]\,[\mathrm{delta}]C_t}$ method, in which:

$$[\mathrm{delta}]\,[\mathrm{delta}]C_t = [\mathrm{delta}]C_{t,\,\mathrm{sample}} - [\mathrm{delta}]C_{t,\,\mathrm{control}} \qquad (1)$$

Here, $[\mathrm{delta}]C_{T,\mathrm{sample}}$ is the C_t value for any experimental animal normalized to the endogenous housekeeping gene and $(\delta)C_{t,\ \mathrm{control}}$ is the C_t value for control animals also normalized to the endogenous housekeeping gene. For each gene and time point, the expression levels were calculated on the basis of triplicates.

Histological Assessment

Infarct size was measured in 15 coronal sections from each forebrain (200-μm apart) stained with cresyl violet. Brain

injury score was calculated from the cresyl violet-stained sections and sections stained with TUNEL and immunohistochemistry for the microglial activation marker 5C6 $\alpha M\beta 2$ expression as described previously,[33] the tissue sections were scored blindly. Overall extent of injury was quantified using infarct size as described previously.[33] For quantitative immunohistochemistry, sections belonging to the same experiment were stained together at the same time to prevent differences in staining intensity as described before.[30] Antibodies, their source, dilutions and the requirement for acetone pretreatment are shown in Table 1. Stained sections were scanned using a Sony AVT-horn video camera and imported into Optimas 6.2 image analysis software. The mean and standard deviation of the optical luminosity values (OLVs; RGB 0–255) were measured in the cortex, hippocampus, thalamus and striatum. The regional raw staining intensity was determined for each section of each brain using the mean ± s.d. algorithm as described before.[30,34] The background staining intensity was measured using the same algorithm and the final staining intensity was calculated by the difference of the raw antibody staining intensity and the background staining intensity. For statistical analysis, the mean of the staining intensity for brain regions for identically treated animals was calculated for endotoxin-treated and control groups.

RESULTS

Survival following Endotoxin +/− HI Insult

To determine the optimal dose and timing of endotoxin in the Rice-Vannucci model of HI insult, we first explored the effects of Lipopolysaccharide (055:B5 *E.* coli lipopolysaccharide/LPS) on 48-h survival of 7-day-old mice. Intraperitoneal application of LPS at a dose of 0.5–5 μg/g body weight was associated with 100% survival; 10 μg/g with that of 93% (14/15); and none of the five animals survived 20 μg/g (Figure 1a).

Animals that underwent HI insult were much more sensitive to pretreatment with LPS. By itself, carotid occlusion and 30-min exposure to 8% oxygen, beginning 2 h after occlusion, was not associated with 48-h loss ($n=5$). However, combination with HI insult rapidly resulted in increasing lethality. Pretreatment with 0.1 μg/g LPS 4 h before carotid occlusion was associated with survival of five out of six, 4/6 at 0.3 μg/g, 1/4 at 1 μg/g and 0/4 at 2 μg/g, with last two dosages showing significant difference to the LPS alone controls in the χ^2-test ($P<0.02$) (Figure 1a). As the next step, we examined the effects of the time interval between pretreatment with LPS and HI insult. As shown in Figure 1b, application of LPS together with, or 4 h preceding the insult was associated with a trend toward reduced, and at 12 and 24 h toward improved survival, even though the numbers did not reach statistical significance ($P=0.08$ in χ^2-test).

Time Course of Endotoxin Pretreatment Before HI Insult

To establish the interval that results in maximal histological brain injury, we next examined the infarct size in animals

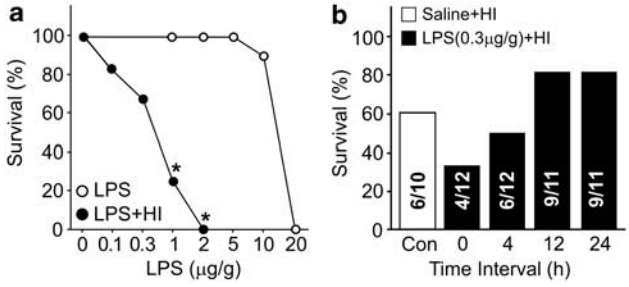

Figure 1 48-h survival following treatment with LPS and Rice-Vanucci model of hypoxic ischemic (HI) insult in postnatal day 7 (P7) mice. (**a**) Dose response to LPS given alone (empty circles) and 4 h before 30-min hypoxia (filled circles). LPS alone becomes lethal at 20 μg/g body weight, together with HI due to carotid occlusion and hypoxia; none of the animals survived at a dose higher than 1 μg/g. *$P<0.02$ in χ^2–test, comparing LPS *vs* LPS and HI. Group size: LPS alone—$n=5$ for all points except 10 μg/g (15), and $n=4$–5 for LPS and HI. (**b**) Effects of time interval between injection with LPS and HI insult. There is a tendency toward reduced survival at short intervals (0–4 h), but this only borders on significance $P=0.08$ in χ^2-test. Con—control animals without LPS injection. The number of surviving animals and total group size (10–12 per group) are shown on the bars.

pre-treated with 0.3 μg/g LPS 0–24 h before carotid occlusion followed by exposure to 8% oxygen for 30 min at P7.

By itself, 30 min HI insult without addition of LPS resulted in variable and sometimes substantial neuronal loss in the ipsilateral pyramidal cell layer of hippocampal CA1-4, with consistent sparing of the dentate gyrus. More moderate losses were also observed in ipsilateral cortex, striatum and thalamus (Figures 2a and d). Compared with the total volume of the ipsilateral cerebral infarct in controls ($1.8\pm0.6\,mm^3$), there was no significant change when LPS was administered at the same time as carotid occlusion ($1.3\pm0.5\,mm^3$, $P=0.87$ for *post hoc* Tukey, $P<0.05$ ANOVA). However, applying it hours earlier (Figures 2a and b) resulted in a gradual increase ($3.9\pm0.4\,mm^3$ at 4, $8.3\pm2.3\,mm^3$ at 12 and $4.0\pm0.8\,mm^3$ at 24 h), reaching significant levels over control and 0 h time points at 12 h ($P<0.05$ for *post hoc* Tukey).

Similar changes were also observed when volume loss was recorded as percent of the contralateral hemisphere (Figure 2b), but there was less inter-animal variability, with a significant increase at 4, as well as at 12 h, compared with the control and 0-h time points ($P<0.05$ for ANOVA and *post hoc* Tukey). Because of this lower variability, we routinely also examined tissue loss as percent of the contralateral brain region. As shown in Figure 2d, this global trend was also observed across all the four forebrain regions in terms of cerebral infarct ($P<0.05$, ANOVA, Tukey). A similar trend was also observed for the injury score in hippocampus, cortex, striatum and thalamus, but did not reach statistical significance because of a higher degree of variance (Figure 2c). However, a 4- or a 12-h pretreatment with LPS also led to a consistent increase in αM integrin and Nissl injury score in the white matter of the ipsilateral external capsule ($P<0.05$, ANOVA, Tukey).

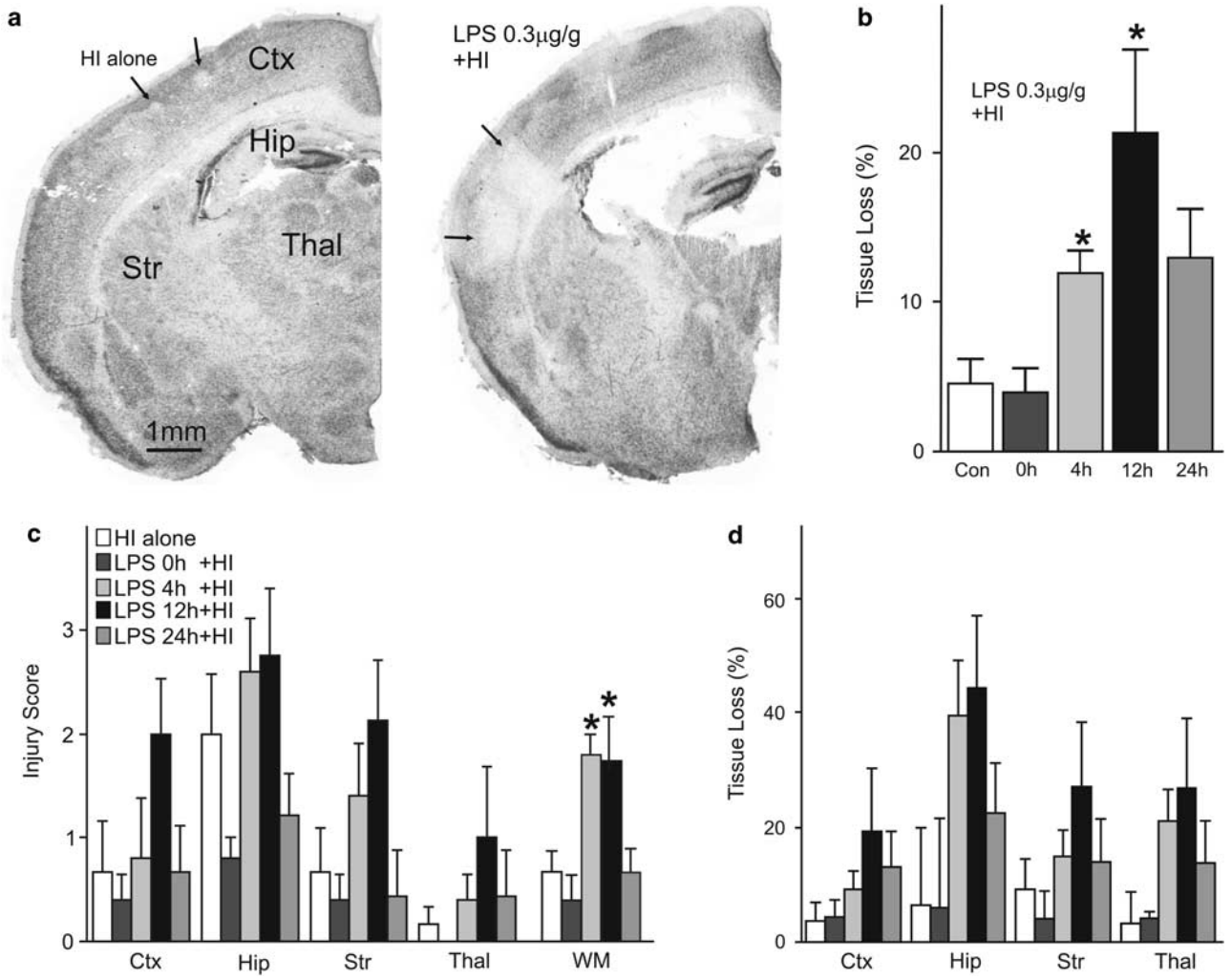

Figure 2 Effects of LPS, and LPS timing on neonatal HI brain damage. (**a**) Pretreatment with 0.3 μg/g LPS 12 h before HI insult (right) strongly increases overall brain damage, compared with 30-min HI alone (left), in Nissl-stained coronal forebrain sections. Note the small foci of cortical cell loss (arrows) on the left and much greater areas of necrotic tissue loss on the right. (**b**) Effect of time interval between LPS and HI insult on forebrain hemisphere tissue loss, as percent of contralateral hemisphere (mean ± s.e.m., $n = 5$–9 animals per group). Note the maximal effect with the 12 h interval. *$P < 0.05$ in ANOVA and *post hoc* Tukey, compared with the control (con) without LPS, and the 0-h LPS group. (**c**, **d**) Effects of combined LPS/HI insult on regional tissue injury score (**c**) and regional tissue loss, as percent of contralateral brain region (**d**). Regional variability was higher than across the entire hemisphere, but there was consistent trend with strongest damage at the 12-h interval. Abbreviations: Ctx—cerebral cortex, Hip—hippocampus, Str—striatum, Thal—thalamus, WM—subcortical white matter (external capsule). Scale Bar: 1 mm.

Gene Expression Following Systemic Endotoxin Application

To explore the molecular signals that lead to enhanced brain injury we next used custom designed Applied Biosystems 384-well Taqman microarray to measure mRNA expression for a selection of cytokines, chemokines and adhesion molecules in P7 mouse forebrain 2–24 h after intraperitoneal injection of 0.3 μg/g LPS.

Compared with controls that were set at 0 on the log(2) scale in Figures 3a and b, the microarrays showed increased mRNA levels for the pro-inflammatory cytokines TNFα, IL1β and IL6, cell adhesion molecules E-Selectin, P-Selectin and ICAM1, and the chemokine CXCL1. IL10, IL12β, IL23α, TGFβ and VCAM1 were unaffected; CCL2 showed a trend toward increase at 2 h, but did not reach statistical significance ($P = 0.07$, ANOVA). In general, LPS-affected cytokines, chemokines and adhesion molecules showed a maximum at 2 h ($P < 0.05$, ANOVA, Tukey); IL1β, CXLCL1 and ICAM1 also showed a significant increase at 12 h, and P-Selectin at all three time points.

As the TNF family (TNFα, LTα and LTβ) have a number of overlapping functions, before examining the effect of TNF cluster deletion we determined the levels of TNFα, LTα and LTβ mRNA in the brain by real-time (RT)-PCR with reverse-transcribed cDNA samples 0–24 h after intraperitoneal injection of endotoxin. Compared with controls, there was increased levels of TNFα and LTβ mRNA 2, 4 and 24 h

after intraperitoneal endotoxin injection, this increase was statistically significant at 4 h ($P<0.05$ ANOVA, Tukey); 12 h after LPS there was no difference in the level of TNFα and LTβ mRNA compared with control (Figures 3c and e). Although there was also a trend toward increased expression of LTα mRNA within the brain at 2 and 12 h, but not at 4 and 24 h after intraperitoneal endotoxin, this did not reach statistical significance (Figure 3d).

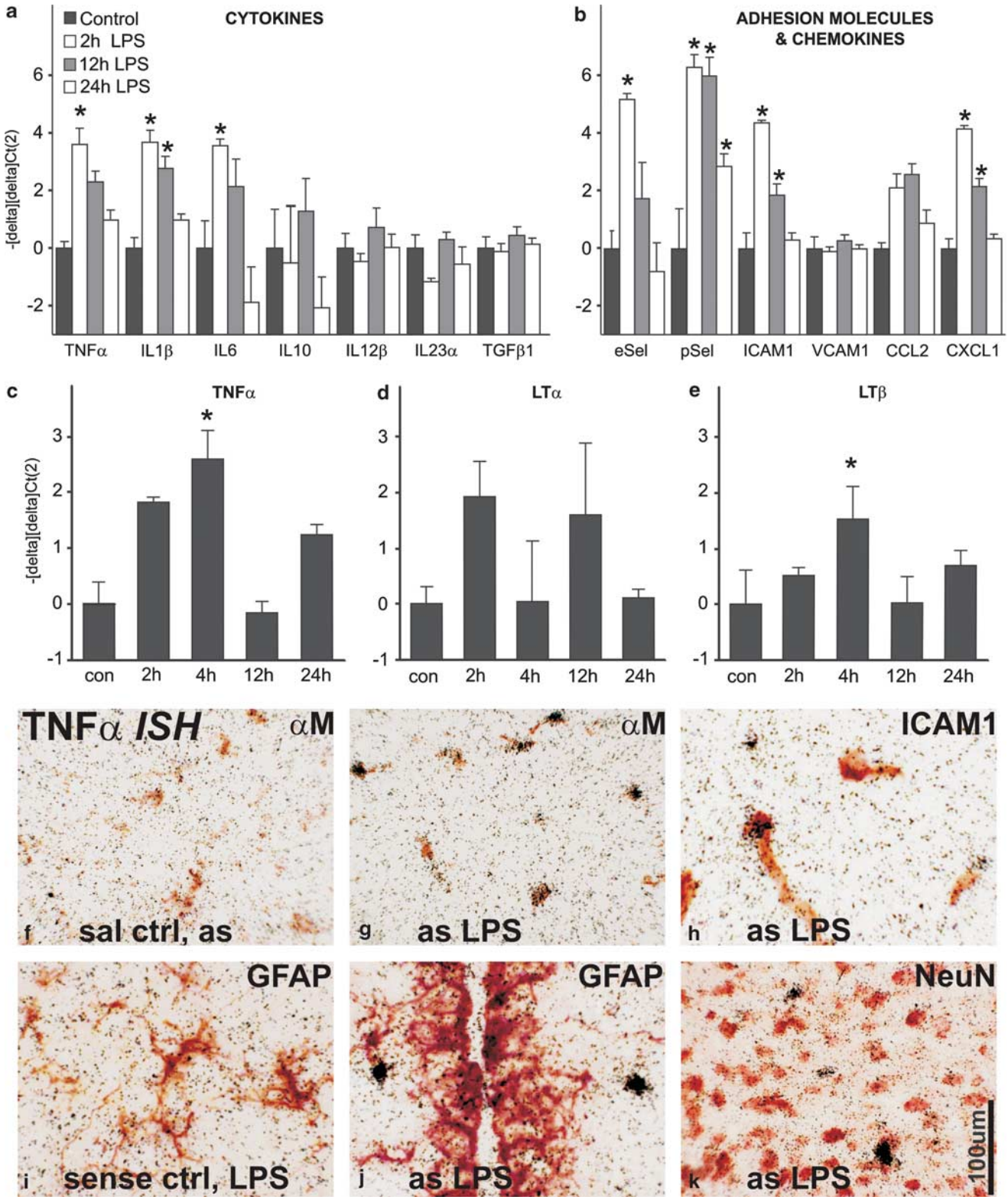

Combined Immunohistochemistry and ISH after Systemic Endotoxin

Because activated microglia/macrophages are an established source of pro-inflammatory cytokines, including TNFα,[35–37] we next explored the cellular localization of the mRNA encoding TNF cluster cytokines 4 h following intraperitoneal injection of 0.3 μg/g LPS. As shown in Figures 3g and h, ISH confirmed strong expression of TNFα mRNA in the P7 mouse forebrain on αM+ brain microglia (Figure 3g), as well as in cells associated with the ICAM1+ blood vessels (Figure 3h). There was no apparent colocalization with the glial fibrillary acidic protein (GFAP)+ astrocytes (Figure 3j) or with the NeuN+ cortical neurons (Figure 3k). Control animals injected with saline showed no prominent clustering of silver grains over the αM+ brain microglia (Figure 3f) or the neighboring blood vessels (not shown). No specific signal was observed using sense TNFα riboprobe. Figure 3i shows this lack of the mRNA signal in combination with the astrocyte GFAP immunolabeling, unlike Figure 3j, which shows clearly labeled clusters of silver grains on the GFAP– cells. The signals for LTα and LTβ were also below the detection level (not shown).

Role of the TNF Family in Endotoxin-Mediated Sensitization to HI Insult

To determine the role of TNF cluster cytokines in the mechanism of endotoxin-mediated senitization to HI insult, we next examined the effect of complete TNF cluster (TNFc) deletion on the infract size. Neonatal mice were obtained as offsprings of crossing heterozygotes (TNFc+/−) with heterozygotes, pre-treated with 0.3 μg/g LPS in isotonic saline 6.5 days after birth, followed by carotid occlusion and exposure to 8% oxygen for 30 min at P7, the latter timed to occur at 12 h after the endotoxin injection. Control littermates were injected with isotonic saline alone, 12 h before the HI insult. In total, 74 out of 109 animals (68%) survived the insult protocol for 48 h. Of the 74 surviving animals, 14 (19%) carried both copies of the TNF cluster (wild type), 42 (57%) were heterozygotes and 18 (24%) were knockouts, with a homozygous deletion for the TNF cluster, ie not significantly different to the expected Mendelian 1:2:1 distribution ($P=0.41$ in χ^2-test). In the following studies we concentrated on the wild-type group and its homozygously null littermates, to detect the effects of presence or complete absence of the TNF cluster cytokines.

The two wild-type (saline *vs* LPS) and the two matching knockout groups were first explored with respect to overall and regional relative infarct size, as percent of forebrain on the contralateral side, and the effects of cluster deletion and pretreatment with LPS; all changes were assessed using unpaired two-tailed *t*-test. As shown in Figure 4a, there was no significant difference in the infarct size between the wild-type genotype ($3.1\pm0.4\%$, $n=8$) and knockout mice ($1.4\pm0.7\%$, $n=4$) after control pretreatment with saline ($P=0.79$).

In wild-type mice, pretreatment with LPS resulted in a significant increase in the overall forebrain infarct size ($P<0.05$), from $3.1\pm0.4\%$ ($n=8$) in animals injected with saline alone to $22.5\pm3.3\%$ in those pretreated with LPS ($n=6$). Knockout animals showed a slight increase, from $1.4\pm0.7\%$ ($n=4$) for saline, to $4.7\pm0.6\%$ for LPS ($n=14$), but this was not significant ($P=0.58$). When the forebrain regions were analyzed separately (Figure 4b), LPS pretreatment in wild-type animals increased infarct size from 2 to 24% in the cortex ($P<0.05$), and from 5 to 20% in striatum ($P<0.05$). The same trend was seen in the hippocampus 5 to 35% ($P=0.06$) and thalamus 4 to 9% ($P=0.56$), but did not reach statistical significance. Homozygous absence of the TNF cluster resulted in the disappearance of a significant endotoxin-sensitizing effect in all analyzed regions: in the cerebral cortex of 1.4 ± 1.4 *vs* $3.9\pm0.7\%$, hippocampus 9.6 ± 3.5 *vs* $13.2\pm1.7\%$, striatum 3.8 ± 0.5 *vs* $6.3\pm0.3\%$ and thalamus 4.6 ± 1.4 *vs* 3.6 ± 0.7.

This dependence of endotoxin effects on the presence of the genes encoding the TNFc cytokines was also observed in absolute volume: this increased from $0.9\pm0.1\,mm^3$ (WT-saline) to $5.7\pm0.8\,mm^3$ (WT-LPS), but dropped to $1.5\pm0.2\,mm^3$ in the KO-LPS group ($P<0.05$ for changes *vs* the WT-LPS group in ANOVA and *post hoc* Tukey). Similar significant effects were also observed for two of the subregions—cortex and striatum, but did not reach the 0.05 significance level in the ANOVA for hippocampus and thalamus ($P=0.15$ and 0.52, respectively).

Figure 3 LPS-induced mRNA expression for cytokines, chemokines and adhesion molecules: regulation and cellular localization. (**a**, **b**) Taqman microarray detection of amplified forebrain cDNA for TNFα, interleukin 1β (IL1β, IL6, IL10, IL12β, IL23α and TGFβ1 (**a**), and E-Selectin (eSel), P-Selectin (pSel), ICAM1, VCAM1, CCL2 and CXCL1 (**b**), at different time intervals (2–24 h) following intraperitoneal injection of 0.3 μg/g LPS. Forebrain tissue from untreated mice was used as control (con). The Y-axis shows the difference in number of cycles for the onset of exponential increase in DNA fluorescence for amplified cDNA for the 18S rRNA (control RNA) *vs* that for specific amplified signal. The difference in the number of cycles for signal from control forebrains was set as 0. Note the particularly consistent upregulation of messages at the 2-h time point. (**c**–**e**) Real-time PCR detection of mRNA encoding TNF cluster members TNFα (**c**), LTα (**d**) and LTβ (**e**), reconfirming early (2–4 h) upregulation of TNFα and LTβ. Group size: $n=4$ animals per time point; $^*P<0.05$, ANOVA and *post hoc* Tukey for the difference compared with the control group. (**f**–**k**) Combined immunohistochemistry and *in situ* hybridization (ISH) for TNFα mRNA. Note the prominent silver grain clusters representing a strong TNFα signal on a subpopulation of αM+ brain microglia (**g**) and ICAM1+ brain blood vessels (**h**), 4 h after intraperitoneal injection with 0.3 μg/g LPS using antisense (as) riboprobes. There is no colocalization of those silver grain clusters with GFAP+ astrocytes (**j**) or NeuN+ cortical neurons (**k**). Animals injected with saline and counterstained for αM+ immunoreactivity (**f**), showed no prominent clustering of silver grains, (compare with **g**). *In situ* hybridization with sense riboprobe (**i**)—here counterstained for GFAP immunoreactivity—showed, compared with (**j**), a lack of specific signal, but had random low level of non-specific hybridization (individual silver grains) across the tissue section and served as a negative control. Scale Bar: 100 μm.

Effect of Endotoxin Pretreatment on TNF Cluster Gene Expression Following HI Insult

To further assess whether endotoxin- and TNF cluster-mediated effects may occur before or also after the HI insult, TNFα, LTα and LTβ mRNA were also quantified by RT-PCR in the brains of animals 0–24 h after carotid occlusion and exposure to 8% oxygen for 30 min. Animals pretreated with saline showed a rapid increase in TNFα (Figure 5a) and LTβ (Figure 5c), reaching a plateau 2 h following insult. In both cases, animals pre-treated with 0.3 μg/g LPS showed a moderate delay in this upregulation 2–4 h following insult.

In the case of LTα (Figure 5b), the mRNA levels revealed considerable intra-group variation following insult, possibly preventing detection of significant changes. This poor detection of LTα appears because of their low absolute levels; some data points (0 h saline, 24 h LPS) were missing because of insufficient amplification. RT-PCR detection for TNFα and LTβ cDNA reverse transcribed from control forebrain tissue normally required on average 17 amplification cycles above that for 18S rRNA that served as reverse transcription and amplification control; LTα on an average required 23 cycles more than those for the 18S species (data not shown).

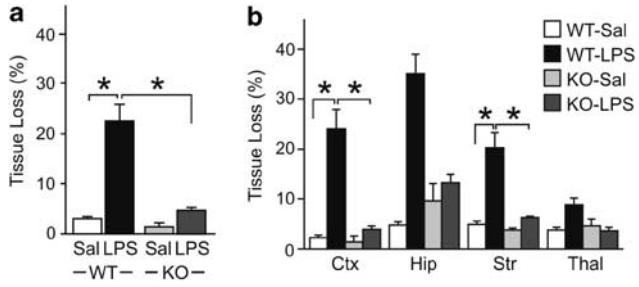

Figure 4 Homozygous absence of the TNF cluster prevents LPS presensitization in neonatal HI insult. (**a**) Forebrain hemisphere tissue loss 48 h following insult, as percent of contralateral hemisphere. Wild-type (WT) animals show significant increase in tissue loss, when injected with LPS 12 h before insult (left two bars) compared with those injected with saline (sal); these effects are absent in the knockout littermates (right). $^*P<0.05$ in Student's *t*-test. (**b**) Similar effects are also apparent in region by region analysis (cortex, hippocampus, striatum and thalamus), reaching statistical threshold for cortex and striatum. Group size: $n=8$ for WT/sal, six for WT/LPS, four for KO/Sal and 14 for KO/LPS.

Time Course of Glial, Leukocyte and Vascular Response to Endotoxin Alone

As significant TNF cluster cytokine elevating effects of endotoxin were only observed in the period between the injection and the HI insult, suggesting that cellular changes during this period are responsible for the sensitization effect, we next explored the effects of endotoxin alone. Increasing the dose of LPS, from 0.1 to up to 10 μg/g followed by 48 h survival, did not reveal any increase in the number of TUNEL+ nuclei compared with saline-treated animals (not shown). Similar lack of histological brain injury was also evident on the cresyl violet-stained sections of the forebrain from the endotoxin-treated animals. However, increasing doses of endotoxin did result in a clear increase in microglial αM (CD11b) integrin subunit immunoreactivity in all forebrain regions assessed, including cortex, hippocampus, striatum and thalamus (Figures 6a–d). This increase was biphasic, with a small elevation at 0.5–2 μg/g, and a larger increase with 5 and 10 μg/g. Interestingly, the highest dose of 10 μg/g also led to the formation of foci of small and rounded αM+ cells (arrows), especially in the cerebral cortex and thalamus (compare Figure 6d with Figures 6a–c).

Because previous reports showed that high levels of peripheral endotoxin can lead to strong brain influx of αM+ neutrophil granulocytes,[14,38] we first wanted to determine whether these rounded αM+ cells were transformed microglia/macrophages or granulocytes, through a double labelling for αM-IR with specific markers for macrophages (ionized calcium-binding adaptor protein 1 (IBA1)) and granulocytes (endogenous peroxidase, EP) in animals treated with 10 μg/g LPS. As shown in Figures 6f–n, about half of the rounded αM+ cells were indeed negative for IBA1-IR (F-H) and positive for EP (I-K). Co-staining with DAPI revealed particularly strong nuclear fluorescence in most EP+ cells (Figures 6h, k and n) and finally, double staining for EP and IBA1 showed the labelling on two non-overlapping cell populations of EP+ granulocytes and IBA1+ brain microglia/macrophages (Figures 6l–n, confirming the presence of the strongly DAPI+, EP+, αM+ and IBA1− granulocytes. However, this massive influx of EP+ granulocytes was only observed with the highest survivable dose,

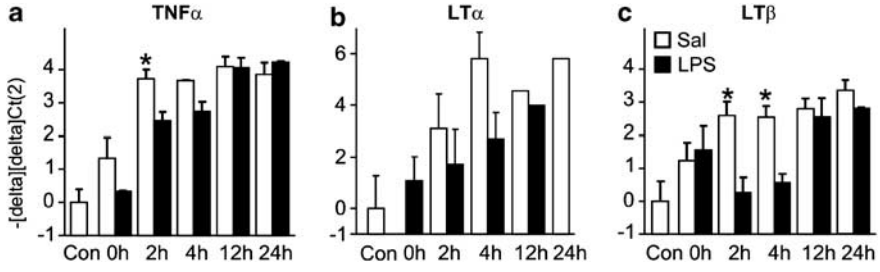

Figure 5 TNFα (**a**), LTα (**b**) and LTβ (**c**) mRNA expression following the HI insult, real-time PCR. The Y-axis shows the difference in number of cycles for the onset of exponential increase in DNA fluorescence for amplified cDNA for the 18S rRNA (control RNA) *vs* that for specific amplified signal. The difference in the number of cycles for signal from control forebrains was set as 0. Animals pretreated with 0.3 μg/g LPS (filled bars) show a delay in full upregulation of TNFα and LTβ mRNAs, compared with saline-injected controls (empty bars). $^*P<0.05$ in Student's *t*-test, $n=4$ animals per group.

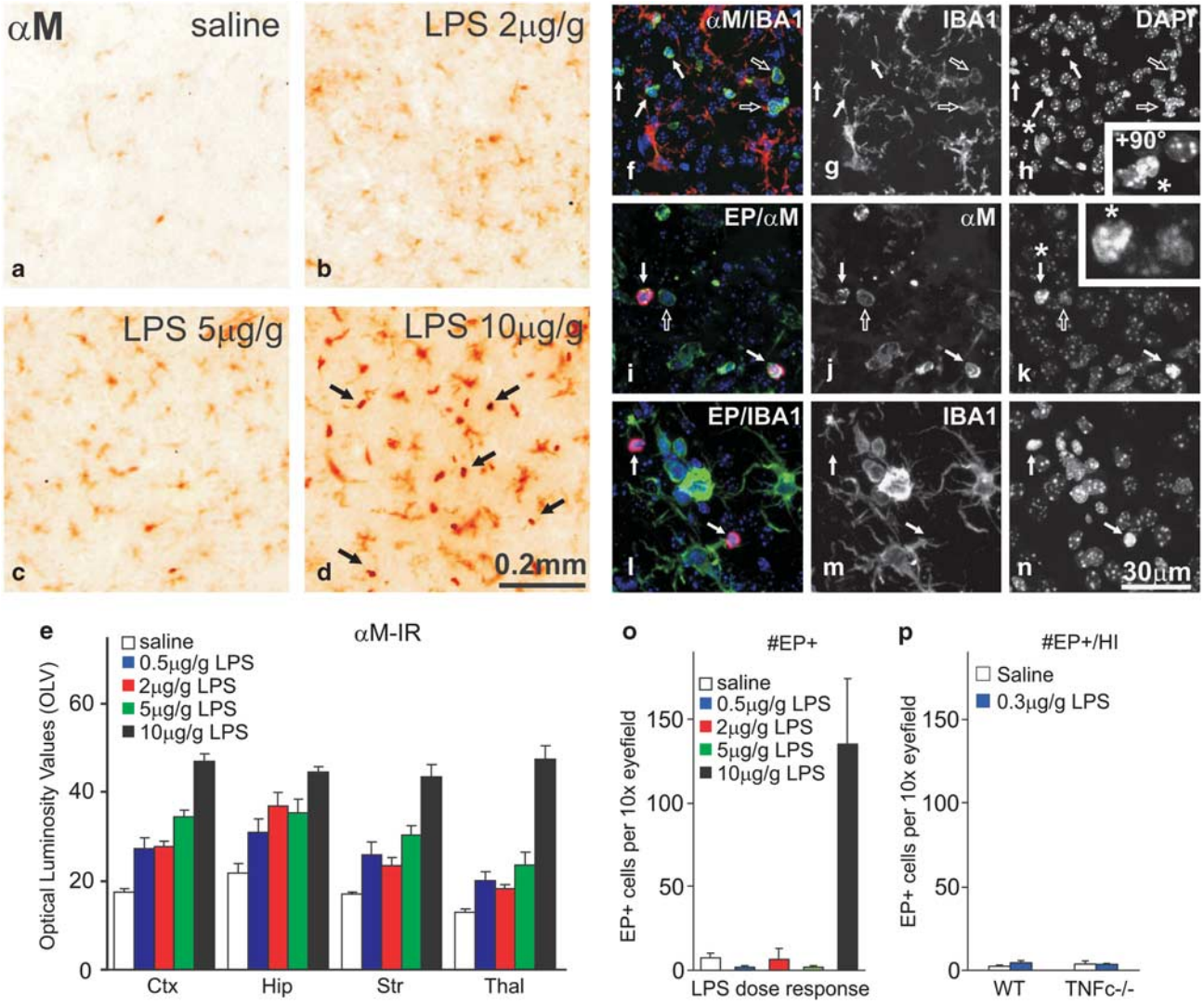

Figure 6 LPS alone induces microglial activation and leukocyte recruitment. (**a**–**e**) Dose response effects on the microglial αM immunoreactivity in cerebral cortex (**a**: saline, **b**: 2 μg/g, **c**: 5 μg/g, **d**: 10 μg/g LPS), and quantification of overall immunoreactivity (**e**) in cortex, hippocampus, striatum and thalamus, 48 h after intraperitoneal injection. The Y-axis in (**e**) shows immunostaining in Optical Luminosity Values (OLVs). Note the gradual increase in staining in all four regions (**e**), as well as the appearance of rounded, αM+ cells at the highest, 10 μg/g dose (**d**). Scale Bar (**a**–**d**): 0.2 mm. (**f**–**p**) Cellular identification (**f**–**n**) and recruitment dynamics (**o**, **p**) of endogenous peroxidase (EP) positive granulocytes in cerebral cortex. (**f**–**n**) Fluorescence triple staining for αM, EP and/or the microglial/macrophage marker IBA1, combined with nuclear DAPI counterstain, to resolve cellular identity of small, rounded, αM+ cells. The triple staining is shown on the left (**f**, **i**, **l**); in (**f**) αM fluorescence is in green and IBA1 in red, in **i**: EP is in red and αM in green, in (**l**) EP is in red and IBA1 in green. Second antibody staining is shown in the middle (**g**, **j**, **m**) and nuclear counterstain—DAPI—in the right column (**h**, **k**, **n**). Rounded αM+ cells consist of at least two distinct populations that are IBA1− (filled arrows) and IBA1+ (empty arrows) in rows **f**–**h**, and EP+ (filled arrows) or EP− (empty arrows) in rows **i**–**k**. Rows **l**–**n** show that double labeling for EP and IBA1 results in no colocalization for the two, cell type-specific markers. As shown in the right column (**h**, **k**, **n**), the αM+ EP+ IBA1− cells also have a more intense nuclear DAPI fluorescence. The inserts in **h** and **k** correspond to higher magnification of nuclear profiles marked by the asterisks. The insert in H is rotated clockwise, by 90°. Scale Bar (**f**–**n**): 30 μm, inserts—10 μm. A color version of 6G-N is shown in Supplementary Figure 2. (**o**, **p**): Massive entry of the small, round, EP+ cells into cerebral cortex is only observed at the highest, 10 μg/g dose after LPS alone (**o**). Saline, 0.5, 2 or 5 μg/g LPS groups did not differ in terms of Ep+ cell density (same color coding as in **e**). In the presence of HI insult (**p**), 12 h previous application of 0.3 μg/g LPS or homozygous deletion of the TNF cluster had no significant effect.

of 10 μg/g LPS. As shown in Figure 6o, a small number of EP+ cells (× 3–7/10 eyefield) were already present in naive, P7 brain and 12 h pretreatment with 0.5–5 μg/ml LPS did not lead to any noticeable increase. Moreover, similar levels of EP+ cells were also observed in wild-type mice, as well as their littermates lacking both gene copies of the TNF cluster, following pretreatment with 0.3 μg/g LPS, as well as in the control groups, following injection of saline (Figure 6p).

As the preliminary study shown in Figures 6a–e revealed a noticeable increase in microglial αM staining with moderate concentrations of 0.5–2 μg/g LPS, we next focused on the glial and vascular response 4–24 h following intraperitoneal

injection of the comparatively low, but standardly used sensitizing dose of 0.3 μg/g LPS. Quantification of the overall immunoreactivity for α5, α6, αM and αX integrins, adhesion ligands ICAM1 and VCAM1 and intracellular adapter molecules IBA1 and GFAP using staining intensity calculated from OLVs (Figures 7a–h) revealed a clear increase ($P<0.05$, Student's *t*-test) in the immunoreactivity for vascular ICAM1 (Figures 7a, i and j) and microglial αM (Figures 7c, k and l), as well as for the mixed microglia/vascular staining pattern for the α6 integrin subunit (Figures 7f, m and n). In the case of ICAM1 and αM, the staining appeared elevated at both early time points—4 and 12 h—but reached statistical significance at the 4 h time point for ICAM1, and 12 h for αM, with borderline *P*-values for the other time point ($P=0.06$ and 0.13 for ICAM1 and αM, respectively). In the case of the α6-integrin subunit, a significant increase was first observed 24 h after LPS injection. No significant change in immunoreactivity was observed for VCAM1 (Figure 7b), αX (Figure 7d), α5 (Figure 7e), IBA1 (Figure 7g) or GFAP (Figures 7h, o and p) at any one of the three tested time points.

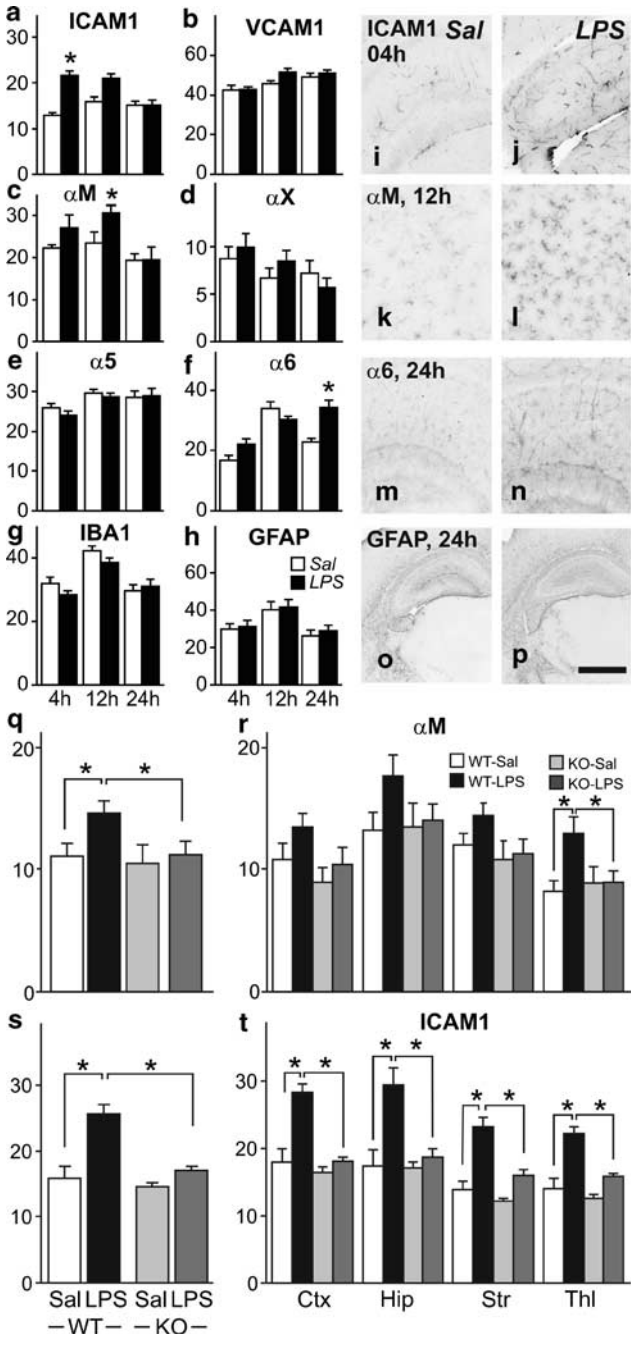

Figure 7 Effects of LPS alone and TNF cluster deletion on cellular activation markers. (**a**–**p**) Quantification of overall forebrain immunoreactivity (**a**–**h**) and histological localization in cerebral cortex (**i**–**p**) of glial and vascular activation markers ICAM1 (**a**, **i**, **j**) and VCAM1 (**b**), the integrin subunits αM (**c**, **k**, **l**), αX (**d**), α5 (**e**) and α6 (**f**, **m**, **n**), and intracellular adapter molecules IBA1 (**g**) and GFAP (**h**, **o**, **p**) following intraperitoneal application of 0.3 μg/g LPS. This dose was sufficient to elicit statistically significant increase of ICAM1 at 4 h, αM at 12 h and α6 at 24 h. All Y-axes show the immunostaining intensity in OLV units. *$P<0.05$ in Student's *t*-test. Scale bar: 0.5 mm in I–N, 1 mm in **o**, **p**. (**q**–**t**) TNF cluster deletion abolishes LPS-induced overall (**q**, **s**) and regional (**r**, **t**) immunoreactivity for the microglial αM integrin subunit (**q**, **r**) and endothelial ICAM1 (**s**, **t**). The overall immunoreactivity in **q** and **s** (in OLV) was calculated from averages across all the four brain regions (cortex, hippocampus, striatum, thalamus) for each individual animal. Note the consistent increase in both types of immunoreactivity, 12 h following 0.3 μg/g LPS (compared with saline, Sal) in wild-type animals (WT), and its absence in the TNF cluster knockouts (KO). *$P<0.05$ in Student's *t*-test.

Effects of TNF Cluster Deletion on Endotoxin-Mediated Cellular Activation

To demonstrate whether the microglial activation and vascular endothelial upregulation are important in the observed sensitization to subsequent HI insult, we also explored whether deletion of the TNF cluster altered these responses following endotoxin application. In total, 63 animals at postnatal day 7 were sequentially allocated to receive 0.3 μg/g LPS in saline or saline alone, without previous knowledge of their genotype. All animals survived to perfusion at 12 h, and then stained for αM and ICAM1 immunoreactivity, in the wild-type and homozygously deficient mice. *Post hoc* genotyping revealed 19 wild-type (30%), 16 knockout (25%) and 28 heterozygote animals (44%), ie again not significantly different to the expected Mendelian 1:2:1 distribution ($P=0.59$ in χ^2-test).

In wild-type animals ($n=9$), LPS application caused a significant, 35–50% increase in the overall, αM (Figure 7q) and ICAM1 immunoreactivity (Figure 7s) across all the four affected forebrain regions (cortex, hippocampus, striatum and thalamus), compared with saline controls ($n=10$, $P<0.05$ for αM and <0.01 for ICAM1). In contrast, littermate animals with homozygous deletion of the TNF cluster showed just a 5–10% increase ($n=6$ and 10, for saline and LPS, respectively), which was not statistically significant.

Moreover, LPS-treated knockouts showed clear and significant lower overall αM and ICAM1 immunostaining than their wild-type siblings ($P<0.05$ for αM and <0.01 for ICAM1) (Figures 7q–t). Region by region analysis for ICAM1 in cortex, hippocampus, striatum and thalamus showed significant changes in all the four regions (Figure 7t). Similar, but more moderate changes were also observed in the case of αM, reaching significant differences for thalamus (Figure 7r), with borderline trends for the cortex ($P=0.11$), hippocampus ($P=0.18$) and striatum ($P=0.12$).

As previous studies showed that LPS will (a) induce iNOS and COX2 on activated macrophages and blood vessels,[39–41] and as (b) the presence of these enzymes will affect the extent of the HI insult,[42,43] we next wanted to determine, whether the protein immunoreactivity level for these enzymes is affected by the comparatively moderate LPS dose used in this study and by the presence or absence of the TNF cluster of cytokines. As shown in Supplementary Figures 1A, G and K, HI insult in the following presensitization with LPS was associated with a higher number of iNOS immunoreactive, rounded macrophage-like cells in the ipsilateral cerebral cortex (33 ± 44 per $\times10$ eyefield, $n=6$), an effect significantly reduced to 5 ± 2 ($n=7$) in the absence of both TNFc genes ($P<0.05$). A similar trend was also observed for COX2, but this did not reach statistical significance, possibly due to relatively strong inter-animal variation in the number of COX2+ cells (Supplementary Figures 1B, O and S). In contrast, there was very little difference in the number of the few rounded iNOS+ or COX2+ cells ($\times3$–6/10 eyefield) on the contralateral, non-occluded side or in the right or left cerebral hemisphere of mice only exposed for 12 h to LPS alone. Interestingly, the overall immunoreactivity for iNOS and COX2, and the pattern of vascular staining showed slightly higher levels in mice injected with LPS and lacking both gene copies of the TNF cluster (Supplementary Figures 1C, D and I and M and Q), but these changes only bordered on statistical significance ($P=0.052$ for iNOS, and $P=0.11$ for COX2, respectively).

DISCUSSION

Although presence of fetal and neonatal infection, high levels of circulating TNFα and specific single-nucleotide polymorphisms for LTα are all associated with enhanced risk of cerebral palsy,[25,26] the direct molecular mechanisms causing perinatal brain damage and ensuing neurological deficits are just beginning to be understood. As shown in the current study, the endogenous TNF cluster cytokines are critical for mediating the sensitizing effects of bacterial breakdown product endotoxin in the mouse model of neonatal HI brain damage. Here, pretreatment with moderate doses of LPS (0.3 μg/g) resulted in severe synergistic tissue damage across the affected ipsilateral forebrain, and pre-exposure to 2 μg/g combined with HI insult produced a uniformly lethal effect not observed following the vascular insult or endotoxin alone.

On the cellular and molecular level, exposure to 0.3 μg/g LPS alone was associated with strong activation of brain blood vessel endothelia and local microglial cells, as well as significant induction of TNFα and LTβ, and a trend toward higher levels of LTα, the three components of the TNF cluster. Although LPS also resulted in a strong upregulation of inflammation-associated cytokines IL-1β and IL6, chemokines, such as CXCL1 and CCL2, and adhesion molecules E-Selectin, P-Selectin and ICAM1, deletion of the TNF gene cluster completely abolished endotoxin-mediated increase in the volume of cerebral infarct. The same deletion also prevented endothelial and microglial activation, exemplified by the increase in ICAM1 and αM, following application of LPS alone, suggesting the involvement of these cell types in bringing about the LPS-mediated sensitization to neonatal brain injury.

Infectious and inflammatory stimuli can and sometimes will result in brain injury. These effects can be direct, following infection alone, or indirect, by enhancing brain injury following trauma, neurodegenerative disease, stroke or other forms of HI insult, and may involve many different signals. In a large gene expression study of postnatal rat, systemic application of LPS, the endotoxin breakdown product of Gram-negative bacteria, resulted in an upregulation of some 1500 genes in the affected brain, including components of immune and inflammatory responses, and cell death pathways.[44] As shown in the current study, in mice, systemic LPS is also associated with a strong mRNA increase in TNFα, LTβ, IL1β, IL6, CXCL1, E-Selectin, P-Selectin and ICAM1, as well as a trend toward increased LTα. The maxima in their observed gene expression profiles, at 2–4 h, correspond to the opening of the window of sensitization detected in the current study (Figure 2), from approximately 4–12 h following application of LPS. Similar window of sensitization was also observed in the postnatal rat, in which LPS pretreatment at 2 h did not, and at 6 h did enhance the HI insult.[45] Surprisingly, the 12 h (and 24 h) time gap between LPS and HI insult appeared to show a tendency toward improved overall survival, compared with the 0 h and 4 h time points, despite the clearly bigger infarct volume. Although the survival effects did not reach statistical significance ($P=0.08$ on χ^2-test), it is possible that combined or almost co-synchronous HI insult and endotoxin could produce a particularly untoward systemic effect, for example, on the cardiovascular or respiratory regulation, irrespective of the brain infarct size. This point is also underscored by the differences deletion of TNF cluster had on infarct size—a strongly negative one, compared with that on survival. With regards to the latter, the very similar percentages of TNFc KO surviving the HI insult (24%) and the proportion of TNFc KO in the large group after LPS alone (25%), both at almost exactly $\frac{1}{4}$ of the total population predicted from a Mendelian distribution, do suggest that the effect of TNFc KO on survival is at best small.

Although this is speculative, exposure to endotoxin is associated with several different waves of cytokines and other

inflammatory signals that could be responsible for the differential effects on brain damage *vs* overall survival.[46,47] It is possible that some of these particularly late components, elicited by LPS preconditioning are also responsible for overall enhanced survival, as well as the neuroprotective effects.[45,48] Significantly, presensitization with LPS in the current study did not cause a synergistically higher TNFα and LTβ mRNA levels in the hours after the HI insult. In fact, Figures 5a and c shows that in during the early phase after HI-insult, LPS-pretreated animals actually had lower cytokine mRNA levels, suggesting that the LPS→TNF cluster cytokine-mediated effects were already executed during the presensitization phase itself.

At the moderate concentrations of LPS, at 0.3 μg/g or below, ie the presensitizing concentration used in the current study, endotoxin signaling appears primarily mediated via CD14 and TLR4; downstream components include IRF, MyD88 and NF-kappaB, and also the AP-1 and egr-1 transcription factors.[49–51] In previous studies, these moderate concentrations were sufficient to evoke cytokine synthesis—IL1β, IL6, TNFα, interferon-γ etc,[17,52,53] and also elicit pronounced stress and febrile response, reduction in feeding and weight loss.[54,55] As shown in Figure 3, the 0.3 μg/g dose is also enough to produce significant induction of the mRNA encoding inflammation-associated adhesion molecules, chemokines and cytokines, including the TNF cluster of cytokines inside the endotoxin-affected brain. The sensitizing effect of endotoxin, observed at the low to mid-levels in the HI insult in this and in previous studies is typically absent in the LPS hyporesponsive strain C3H/HeJ,[16] in which the TLR4 is inactivated through a single proline to histidine substitution, P712H.[56,57]

Many of the currently detected molecular signals, including E- and P-Selectin, ICAM1, IL1α and β, are also upregulated in adult stroke, and involved in mediating neural injury. For example, inactivation of E-Selectin and P-Selectin has been noted to reduce leukocyte entry and tissue loss, and improves blood perfusion in cerebral ischemia and stroke models.[58–61] Combined deletion of E- and P-Selectin also completely inhibits meningeal extravasation in the interferon-γ induced, sterile meningitis model.[62] Similar effects were also observed for ICAM1[38,59,63] and IL1.[64–66] Selective deletion of the IL1-converting enzyme, needed to activate IL1β, also protects against moderate, but not severe forms of the neonatal hypoxic ischemic insult.[67] However, it appears unlikely that the current presensitization effects by themselves were due to leukocyte entry. Thus, the comparatively moderate LPS levels used to elicit synergistic effects were not associated with enhanced number of granulocytes in the cortical parenchyma, shown in Figure 6f, nor with the presence of rounded, iNOS+ and COX2+ macrophage-like cells following application of LPS alone, or in the contralateral forebrain, following synergistic LPS/HI insult (Supplementary Figure 1).

As in previous studies,[14,38] very high levels of endotoxin were indeed associated with direct influx of endogenous peroxidise+ granulocytes, and the appearance of rounded IBA1+ brain macrophages in the neonatal brain. However, these changes were only present at the highest survivable dose without the additional insult, 1.5 orders of magnitude higher than that required to elicit the pre-sensitization response. Altogether these data point to primary role of local parenchymal response, particularly that of microglia and brain vascular endothelia, a notion reinforced by the specific expression of TNFα in subpopulations of microglial and vascular cells shown in Figures 3g and h. Although current data seem to argue against the involvement of reactive nitrogen species or polyunsaturated acid derivatives in the presensitization response, activated microglial cells do contain a host of potentially neurotoxic compounds, including glutamate and fas ligands,[19] which could decrease the damage threshold to brain hypoxia. LPS presensitization also induced strong expression of endothelial ICAM1 and the microglial αMβ2 integrin. Both molecules subserve cell adhesion; however, they are also strongly involved in phagocytosis and inside-out signaling,[31,68,69] and, for the αMβ2 integrin, have been shown to enhance neonatal neural cell death, via the superoxide ion pathway.[70]

In the case of the TNF cluster of cytokines, exogenous TNFα has been shown to exacerbate focal ischemic injury and blocking endogenous TNFα has been shown to be neuroprotective.[71] Studies using homozygously-bred TNFα-deficient mice suggested protective effect of TNFα in the adult middle artery occlusion model.[72] Similar apparent effects were also present for homozygously-bred mice carrying deletions for TNF receptor type 1 alone[72] and combined with TNFR2.[72,73] To avoid genetic and phenotypic drifts that can occur during homozygous breeding,[74] in the current study we specifically used heterozygously bred mice to generate littermate knockouts and wild types that, by definition, will share the same background. Under these conditions, the TNF cluster of cytokines exerted a clearly detrimental effect.

Although the broader TNF super family currently numbers more than 20 members,[27] the actual 12 kb TNF gene cluster contains only genes encoding three ligands—TNFα, LTα and LTβ—that are highly structurally and functionally related. TNFα exists as either a membrane-bound or soluble homotrimer, and binds to two TNF receptors (TNRFp55 and TNRFp75) that are shared with the secreted homotrimer LTα3. The predominant form of LTβ is a membrane-bound heterotrimer, and, together with LTα, signals through a distinct receptor, LTβR.[23] To explore the effect of TNF group at outset it was necessary to delete all three cytokines, to prevent potential compensation due to functional overlap. In fact, the current study demonstrated the upregulation of TNFα and LTβ, as well as a trend toward increased LTα in the hours following HI insult. Here, deletion of the entire TNF gene cluster, removing TNFα, LTβ and LTα completely abolished endotoxin-mediated increase in the volume of cerebral infarct; thus these cytokines appear critical to this process. LTβ and particularly LTα were overall expressed at lower levels

and generally below the detectability threshold for ISH, but at the moment, we cannot exclude that they contribute to the sensitizing effects. In a future study, it will be important to see whether these effects are due to the presence of one specific cytokine or combination of these three, and whether it is due to its expression in the hematopoetic nor non-hematopoetic component, as has been shown for the LPS signaling at the TLR4 and MyD88 level.[17,53] Although TLR4 and MyD88 null mice are complete inactivations, floxed genes encoding several other components of the LPS signaling pathway, including MAP-kinases and transcription factors, such as AP-1 (Behrens *et al*[75]), are available and so could be used in future studies to selectively delete parts of the pathway in microglia, endothelia or neurons, in order to delineate the cellular sequence of LPS-induced events.

Supplementary Information accompanies the paper on the Laboratory Investigation website (http://www.laboratoryinvestigation.org)

ACKNOWLEDGEMENTS

Giles Kendall was the recipient of the Action Medical Research Training Fellowship (RTF1115), and is a National Institute for Health Research (NIHR) funded Clinical Lecturer. This work was supported by Wellbeing of Women (WoW, PG683/05), Motorneuron Disease (Oct06/6220) and Sport Action Research for Kids (SPARKS, 07UCL02) research charities.

DISCLOSURE/CONFLICT OF INTEREST

The authors declare no conflict of interest.

1. Stanley F, Blair E, Alberman E. Cerebral Palsies: Epidemiology and Casual Pathways. MacKeith: London, 2000.
2. Jacobsson B, Hagberg G. Antenatal risk factors for cerebral palsy, Best Practice & Research. Clinical Obstetrics & Gynaecology 2004;18:425–436.
3. Badawi N, Kurinczuk JJ, Keogh JM, *et al.* Intrapartum risk factors for newborn encephalopathy: the Western Australian case-control study. BMJ 1998;317:1554–1558.
4. Peebles DM, Wyatt JS. Synergy between antenatal exposure to infection and intrapartum events in causation of perinatal brain injury at term. BJOG 2002;109:737–739.
5. Blair E, Stanley F. Issues in the classification and epidemiology of cerebral palsy. Ment Retard Dev Dis Res Rev 2002;3:184–193.
6. Eklind S, Mallard C, Leverin AL, *et al.* Bacterial endotoxin sensitizes the immature brain to hypoxic-ischaemic injury. Eur J Neurosci 2001;13 :1101–1106.
7. Coumans AB, Middelanis JS, Garnier Y, *et al.* Intracisternal application of endotoxin enhances the susceptibility to subsequent hypoxic-ischemic brain damage in neonatal rats. Pediatr Res 2003;53:770–775.
8. Yang L, Sameshima H, Ikeda T, *et al.* Lipopolysaccharide administration enhances hypoxic-ischemic brain damage in newborn rats. J Obstet Gynaecol Res 2004;30:142–147.
9. Xue M, del Bigio MR. Immune pre-activation exacerbates hemorrhagic brain injury in immature mouse brain. J Neuroimmunol 2005;165: 75–82.
10. Wang X, Carmichael DW, Cady EB, *et al.* Greater hypoxia-induced cell death in prenatal brain after bacterial-endotoxin pretreatment is not because of enhanced cerebral energy depletion: a chicken embryo model of the intrapartum response to hypoxia and infection. J Cereb Blood Flow Metab 2007;28:948–960.
11. Weinstein JR, Swarts S, Bishop C, *et al.* Lipopolysaccharide is a frequent and significant contaminant in microglia-activating factors. Glia 2008;56:16–26.
12. Kim H, Koh G. Lipopolysaccharide activates matrix metalloproteinase-2 in endothelial cells through an NF-kappaB-dependent pathway. Biochem Biophys Res Commun 2000;269:401–405.
13. Bohatschek M, Kloss CU, Kalla R, *et al. In vitro* model of microglial deramification: ramified microglia transform into amoeboid phagocytes following addition of brain cell membranes to microglia-astrocyte co-cultures. J Neurosci Res 2001;64:508–522.
14. Cunningham C, Wilcockson DC, Campion S, *et al.* Central and systemic endotoxin challenges exacerbate the local inflammatory response and increase neuronal death during chronic neurodegeneration. J Neurosci 2005;25:9275–9284.
15. Rosenberg GA, Estrada EY, Mobashery S. Effect of synthetic matrix metalloproteinase inhibitors on lipopolysaccharide-induced blood-brain barrier opening in rodents: Differences in response based on strains and solvents. Brain Res 2007;1133:186–192.
16. Lehnardt S, Massillon L, Follett P, *et al.* Activation of innate immunity in the CNS triggers neurodegeneration through a Toll-like receptor 4-dependent pathway. Proc Natl Acad Sci USA 2003;100:8514–8519.
17. Gosselin D, Rivest S. MyD88 signaling in brain endothelial cells is essential for the neuronal activity and glucocorticoid release during systemic inflammation. Mol Psychiatry 2008;13:480–497.
18. Volpe JJ. Neurobiology of periventricular leukomalacia in the premature infant. Pediatr Res 2001;50:553–562.
19. Taylor DL, Jones F, Kubota ES, *et al.* Stimulation of microglial metabotropic glutamate receptor mGlu2 triggers tumor necrosis factor alpha-induced neurotoxicity in concert with microglial-derived Fas ligand. J Neurosci 2005;25:2952–2964.
20. Bal-Price A, Brown GC. Inflammatory neurodegeneration mediated by nitric oxide from activated glia-inhibiting neuronal respiration, causing glutamate release and excitotoxicity. J Neurosci 2001;21:6480–6491.
21. Matute C, Domercq M, Sánchez-Gómez MV. Glutamate-mediated glial injury: mechanisms and clinical importance. Glia 2006;53:212–224.
22. del Zoppo GJ, Milner R, Mabuchi T, *et al.* Microglial activation and matrix protease generation during focal cerebral ischemia. Stroke 2007;38(2 Suppl):646–651.
23. Kuprash DV, Alimzhanov MB, Tumanov AV, *et al.* Redundancy in tumor necrosis factor (TNF) and lymphotoxin (LT) signalling *in vivo*: mice with inactivation of the entire TNF/LT locus *versus* single-knockout mice. Mol Cell Biol 2002;22:8626–8634.
24. Grivennikov SI, Kuprash DV, Liu ZG, *et al.* Intracellular signals and events activated by cytokines of the tumor necrosis factor superfamily: From simple paradigms to complex mechanisms. Int Rev Cytol 2006; 252:129–161.
25. Nelson KB, Dambrosia JM, Grether JK, *et al.* Neonatal cytokines and coagulation factors in children with cerebral palsy. Ann Neurol 1998;44:665–675.
26. Nelson KB, Dambrosia JM, Iovannisci DM, *et al.* Genetic polymorphisms and cerebral palsy in very preterm infants. Pediatr Res 2005;57:494–499.
27. Hehlgans T, Pfeffer K. The intriguing biology of the tumour necrosis factor/tumour necrosis factor receptor superfamily: players, rules and the games. Immunology 2005;115:1–20.
28. Markus T, Cronberg T, Cilio C, *et al.* Tumor necrosis factor receptor-1 is essential for LPS-induced sensitization and tolerance to oxygen-glucose deprivation in murine neonatal organotypic hippocampal slices. J Cereb Blood Flow Metab 2009;29:73–86.
29. Rice III JE, Vannucci RC, Brierley JB. The influence of immaturity on hypoxic-ischemic brain damage in the rat. Ann Neurol 1981;9:131–141.
30. Moller JC, Klein MA, Haas S, *et al.* Regulation of thrombospondin in the regenerating mouse facial motor nucleus. Glia 1996;17:121–132.
31. Hristova M, Cuthill D, Zbarsky V, *et al.* Activation and deactivation of periventricular white matter phagocytes during postnatal mouse development. Glia 2010;58:11–28.
32. Kalla R, Liu Z, Xu S, *et al.* Microglia and the early phase of immune surveillance in the axotomized facial motor nucleus: impaired microglial activation and lymphocyte recruitment but no effect on neuronal survival or axonal regeneration in macrophage-colony stimulating factor-deficient mice. J Comp Neurol 2001;436:182–201.
33. Kendall GS, Robertson NJ, Iwata O, *et al.* N-methyl-isobutyl-amiloride ameliorates brain injury when commenced before hypoxia ischemia in neonatal mice. Pediatr Res 2006;59:227–231.
34. Kloss CU, Bohatschek M, Kreutzberg GW, *et al.* Effect of lipopolysaccharide on the morphology and integrinintegrin immunoreactivity of ramified microglia in the mouse brain and in cell culture. Exp Neurol 2001;168:32–46.
35. Benveniste EN. Inflammatory cytokines within the central nervous system: sources, function, and mechanism of action. Am J Physiol 1992;263:C1–16.

36. Guan J, Bennet L, George S, *et al.* Insulin-like growth factor-1 reduces postischemic white matter injury in fetal sheep. J Cereb Blood Flow Metab 2001;21:493–502.
37. Glezer I, Simard AR, Rivest S. Neuroprotective role of the innate immune system by microglia. Neuroscience 2007;147:867–883.
38. Bohatschek M, Werner A, Raivich G. Systemic LPS injection leads to granulocyte influx into normal and injured brain: effects of ICAM-1 deficiency. Exp Neurol 2001;172:137–152.
39. Nomura Y, Kitamura Y. Inducible nitric oxide synthase in glial cells. Neurosci Res 1993;18:103–107.
40. Minc-Golomb D, Yadid G, Tsarfaty I, *et al. In vivo* expression of inducible nitric oxide synthase in cerebellar neurons. J Neurochem 1996;66:1504–1509.
41. Elmquist JK, Breder CD, Sherin JE, *et al.* Intravenous lipopolysaccharide induces cyclooxygenase 2-like immunoreactivity in rat brain perivascular microglia and meningeal macrophages. J Comp Neurol 1997;381:119–129.
42. Iadecola C, Zhang F, Casey R, *et al.* Delayed reduction of ischemic brain injury and neurological deficits in mice lacking the inducible nitric oxide synthase gene. J Neurosci 1997;17:9157–9164.
43. Iadecola C, Niwa K, Nogawa S, *et al.* Reduced susceptibility to ischemic brain injury and N-methyl-D-aspartate-mediated neurotoxicity in cyclooxygenase-2-deficient mice. Proc NatlAcadNatl Acad Sci USA 2001;98:1294–1299.
44. Eklind S, Hagberg H, Wang X, *et al.* Effect of lipopolysaccharide on global gene expression in the immature rat brain. Pediatr Res 2006;60:161–168.
45. Eklind S, Mallard C, Arvidsson P, *et al.* Lipopolysaccharide induces both a primary and a secondary phase of sensitization in the developing rat brain. Pediatr Res 2005;58:112–116.
46. Wang H, Bloom O, Zhang M, *et al.* HMG-1 as a late mediator of endotoxin lethality in mice. Science 1999;285:248–251.
47. Moldawer LL. Biology of proinflammatory cytokines and their antagonists. Critical Care Med 1994;22:S3–S7.
48. Lin HY, Huang CC, Chang KF. Lipopolysaccharide preconditioning reduces neuroinflammation against hypoxic ischemia and provides long-term outcome of neuroprotection in neonatal rat. Pediatr Res 2009;66:254–259.
49. Takeuchi O, Akira S. Toll-like receptors; their physiological role and signal transduction system. Int Immunopharmacol 2001;1:625–635.
50. Triantafilou M, Triantafilou K. Lipopolysaccharide recognition: CD14, TLRs and the LPS-activation cluster. Trends Immunol 2002;23:301–304.
51. Medzhitov R, Horng T. Transcriptional control of the inflammatory response. Nat Rev Immunol 2009;9:692–703.
52. Singh AK, Jiang Y. How does peripheral lipopolysaccharide induce gene expression in the brain of rats? Toxicology 2004;201: 197–207.
53. Chakravarty S, Herkenham M. Toll-like receptor 4 on nonhematopoietic cells sustains CNS inflammation during endotoxemia, independent of systemic cytokines. J Neurosci 2005;25:1788–1796.
54. Ogimoto K, Harris Jr MK, Wisse BE. MyD88 is a key mediator of anorexia, but not weight loss, induced by lipopolysaccharide and interleukin-1 beta. Endocrinol 2006;147:4445–4453.
55. Wisse BE, Ogimoto K, Tang J, *et al.* Evidence that lipopolysaccharide-induced anorexia depends upon central, rather than peripheral, inflammatory signals. Endocrinol 2007;148:5230–5237.
56. Poltorak A, He X, Smirnova I, *et al.* Defective LPS signaling in C3H/HeJ and C57BL/10ScCr mice: mutations in Tlr4 gene. Science 1998;282: 2085–2088.
57. Qureshi ST, Larivière L, Leveque G, *et al.* Endotoxin-tolerant mice have mutations in Toll-like receptor 4 (Tlr4). J Exp Med 1999;189:615–625.
58. Connolly Jr ES, Winfree CJ, Prestigiacomo CJ, *et al.* Exacerbation of cerebral injury in mice that express the P-selectin gene: identification of P-selectin blockade as a new target for the treatment of stroke. Circ Res 1997;81:304–310.
59. Connolly Jr ES, Winfree CJ, Springer TA, *et al.* Cerebral protection in homozygous null ICAM-1 mice after middle cerebral artery occlusion. Role of neutrophil adhesion in the pathogenesis of stroke. J Clin Invest 1996;97:209–216.
60. Suzuki H, Abe K, Tojo SJ, *et al.* Reduction of ischemic brain injury by anti-P-selectin monoclonal antibody after permanent middle cerebral artery occlusion in rat. Neurol Res 1999;21:269–276.
61. Mocco J, Choudhri T, Huang J, *et al.* HuEP5C7 as a humanized monoclonal anti-E/P-selectin neurovascular protective strategy in a blinded placebo-controlled trial of nonhuman primate stroke. Circ Res 2002;91:907–914.
62. Tang T, Frenette PS, Hynes RO, *et al.* Cytokine-induced meningitis is dramatically attenuated in mice deficient in endothelial selectins. J Clin Invest 1996;97:2485–2490.
63. Kitagawa K, Matsumoto M, Mabuchi T, *et al.* Deficiency of intercellular adhesion molecule 1 attenuates microcirculatory disturbance and infarction size in focal cerebral ischemia. J Cereb Blood Flow Metab 1998;18:1336–1345.
64. Yamasaki Y, Matsuura N, Shozuhara H, *et al.* Interleukin-1 as a pathogenetic mediator of ischemic brain damage in rats. Stroke 1995;26:676–680.
65. Hara H, Friedlander RM, Gagliardini V, *et al.* Inhibition of interleukin 1beta converting enzyme family proteases reduces ischemic and excitotoxic neuronal damage. Proc Natl Acad Sci 1997;94: 2007–2012.
66. Stroemer RP, Rothwell NJ. Cortical protection by localized striatal injection of IL-1ra following cerebral ischemia in the rat. J Cereb Blood Flow Metab 1997;17:597–604.
67. Liu XH, Kwon D, Schielke GP, *et al.* Mice deficient in interleukin-1 converting enzyme are resistant to neonatal hypoxic-ischemic brain damage. J Cereb Blood Flow Metab 1999;19:1099–1108.
68. Ehirchiou D, Xiong YM, Li Y, *et al.* Dual function for a unique site within the beta2I domain of integrin alphaMbeta2. J Biol Chem 2005;280: 8324–8331.
69. Zhou X, Perez F, Han K, *et al.* Clonal senescence alters endothelial ICAM-1 function. Mech Ageing Dev 2006;127:779–785.
70. Wakselman S, Béchade C, Roumier A, *et al.* Developmental neuronal death in hippocampus requires the microglial CD11b integrin and DAP12 immunoreceptor. J Neurosci 2008;28:8138–8143.
71. Barone FC, Arvin B, White RF, *et al.* Tumor necrosis factor-alpha: A mediator of focal ischemic brain injury. Stroke 1997;28:1233–1244.
72. Lambertsen KL, Clausen BH, Babcock AA, *et al.* Microglia protect neurons against ischemia by synthesis of tumor necrosis factor. J Neurosci 2009;29:1319–1330.
73. Bruce AJ, Boling W, Kindy MS, *et al.* Altered neuronal and microglial responses to excitotoxic and ischemic brain injury in mice lacking TNF receptors. Nat Med 1996;2:788–794.
74. Werner A, Martin S, Gutierrez-Ramos JC, *et al.* Leukocyte recruitment and neuroglial activation during facial nerve regeneration in ICAM-1-deficient mice: effects of breeding strategy. Cell Tissue Res 2001;305: 25–41.
75. Behrens A, Sibilia M, David JP, *et al.* Impaired postnatal hepatocyte proliferation and liver regeneration in mice lacking c-jun in the liver. EMBO J 2002;21:1782–1790.